

Metathesis of Olefin-Substituted Pyridines: The Metalated NCN-Pincer Complex in a Dual Role as Protecting Group and Scaffold**

Harm P. Dijkstra,^a Aleksey Chuchuryukin,^a Bart M. J. M. Suijkerbuijk,^a Gerard P. M. van Klink,^a Allison M. Mills,^b Anthony L. Spek,^{b,c} Gerard van Koten^{a,*}

^a Debye Institute, Department of Metal-Mediated Synthesis, Utrecht University, Padualaan 8, 3584 CH Utrecht, The Netherlands

Tel: (+31)-30-2533120, Fax: (+31)-30-2523615, e-mail: g.vankoten@chem.uu.nl

^b Bijvoet Center for Biomolecular Research, Department of Crystal and Structural Chemistry, Utrecht University, Padualaan 8, 3584 CH Utrecht, The Netherlands

^c Address correspondence pertaining to crystallographic studies to this author.
E-mail: A.L.Spek@chem.uu.nl

Received: February 8, 2002; Accepted: April 18, 2002

Abstract: Pincer-palladium(II) and -platinum(II) cations, YCY-M (YCY = [2,6-(YCH₂)₂C₆H₃]⁻; Y = NMe₂, SPh; M = Pd^{II}, Pt^{II}), bound to diolefin-substituted pyridines (3,5- or 2,6-substitution) were successfully synthesized, and subsequently used in olefin metathesis (RCM) as a model study for template-directed synthesis of macrocycles. Especially a 3,5-disubstituted pyridine bound to a NCN-Pt^{II}-center (**5a**) gave a fast metathesis reaction, while the same reaction with the Pd^{II} analogue (**4a**) was much slower and less selective (isomerization products were formed). Furthermore, it was found that 2,6-diolefin-substituted pyridines (**4b**, **5b**, **5c**) gave slow metathesis reactions, which is mainly ascribed to steric hindrance during the ring-closing step. In all cases where prolonged reaction times were required an isomerization process, most likely assisted by cationic pincer-M^{II} species, was observed as a competing reaction. ¹H NMR spectroscopy experiments revealed that pyridines are stronger bound to a cationic NCN-Pt^{II}-center than to its Pd^{II}-analogue. This aspect is of crucial importance when these pincer-pyridine complexes are

applied in metathesis, since free pyridine in solution deactivates the Ru-metathesis catalyst. For the templated construction of macrocycles, a strong M-N(py) bond is also important since it determines the selectivity for the desired product. In addition, these results open a new research field in which organometallic (pincer) complexes are used as protecting groups for strong Lewis-basic groups in catalysis. From failed attempts to prepare macrocycles using hexakis[SCS-Pd^{II}-(**1a**)] complex **14**, and from the results obtained with the monometallic pincer complexes in RCM, it can be concluded that the most suitable candidate for constructing macrocycles should comprise 2,6-diolefin-substituted pyridines bound to a multi-(NCN-Pt^{II})-template. In such a system, intrapyridine metathesis (steric hindrance) as well as isomerization reactions (strong M-N(py) bond) are suppressed.

Keywords: coordination chemistry; olefin-substituted pyridines; pincer-metal protecting group; ring-closing metathesis; template directed synthesis

Introduction

The number of applications of olefin metathesis in organic synthesis has increased rapidly during the last decade.^[1] Especially with the introduction of the well-defined metal-alkylidene catalysts, metathesis chemistry is increasingly being used in organic transformations.^[2] In particular, Grubbs' ruthenium catalyst

[(Cy₃P)₂Cl₂Ru=CHPh] has attracted wide-spread attention due to its ease of handling and tolerance toward many functional groups.^[3] Unfortunately, Lewis-basic functional groups, such as nitriles, amines and pyridines, are not tolerated in the olefin metathesis reaction using this ruthenium catalyst.^[4]

The use of olefin-substituted metal complexes in olefin metathesis has not been investigated in great detail yet. Grubbs, Sauvage and coworkers reported the use of phenanthroline-containing olefins assembled with copper(II) ions in ring-closing metathesis (RCM) to form catenanes.^[5] Furthermore, Gladysz and co-

**Part of this work was presented at the 14th International Symposium on Olefin Metathesis, Boston, August 2001

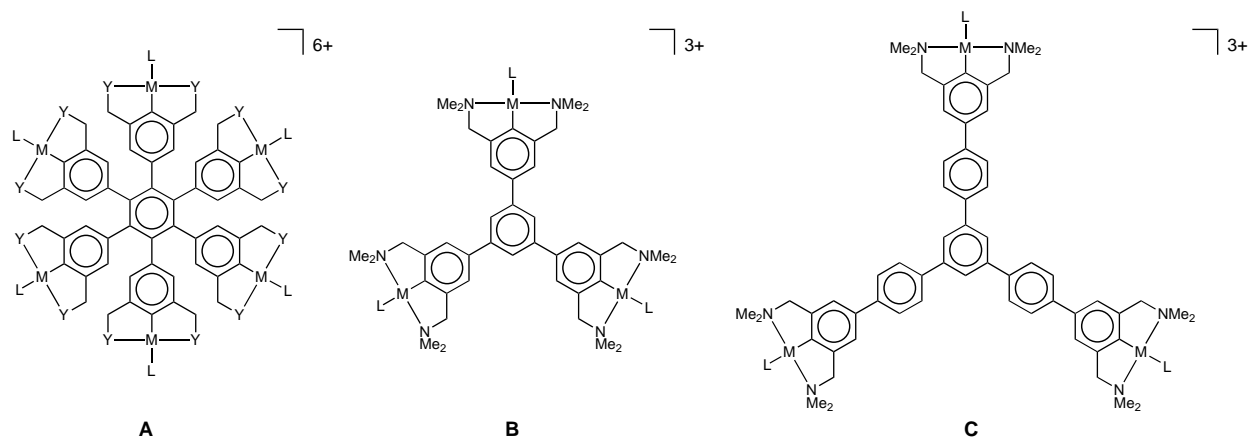
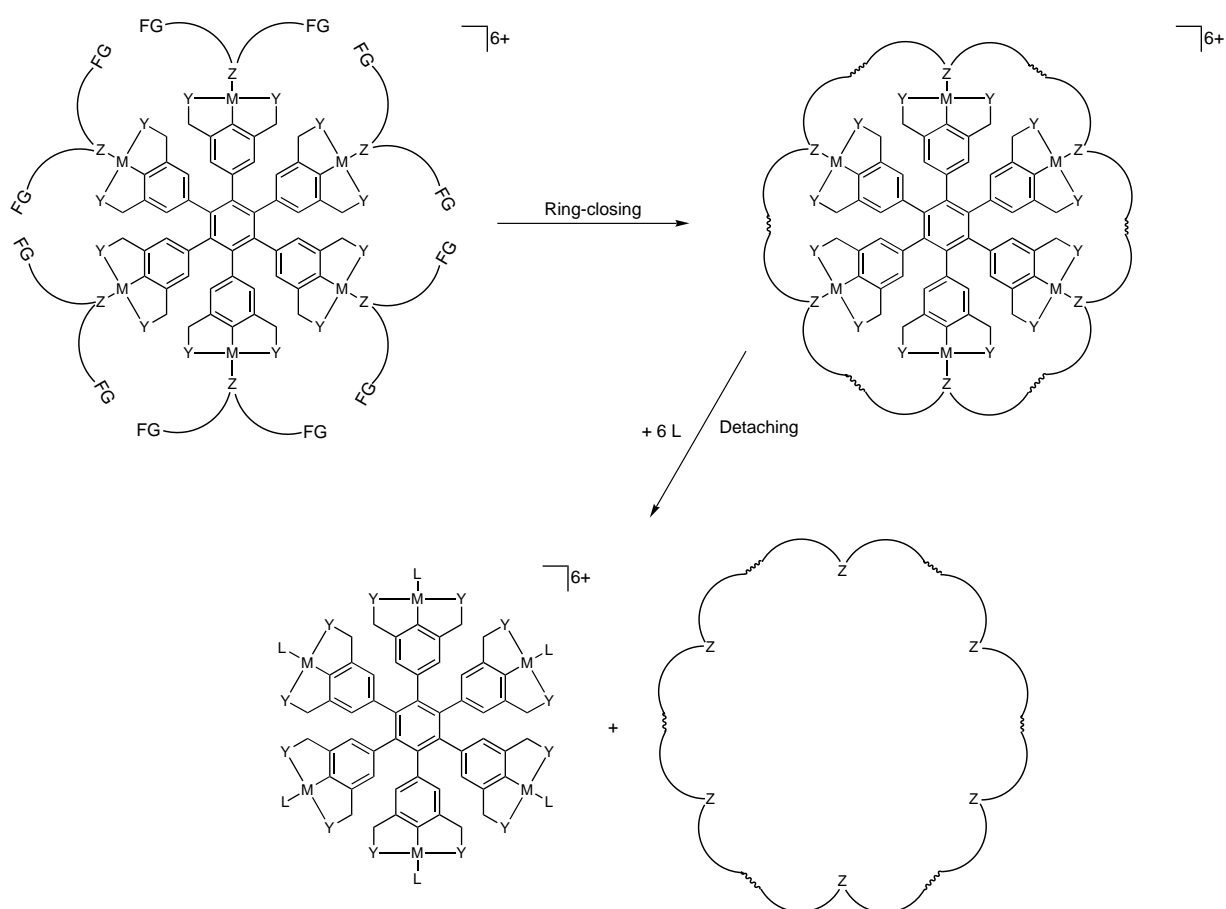


Figure 1. Highly ordered shape-persistent multimetallic materials.

workers reported olefin metathesis in the metal coordination sphere using olefin-substituted phosphine- and sulfur-ligands coordinated to platinum(II), rhenium(II) and tungsten(0) centers.^[6] The application of a 2,6-diolefin-substituted pyridine coordinated to a palladium(II) center in olefin metathesis has also been reported.^[7] In all of these cases the metal ion serves as

the template to preorganize the ligands prior to metathesis in order to construct heterocyclic structures.

Recently, we started to explore the application of shape-persistent nanosize multimetallic materials (**A–C**, Figure 1) as recyclable homogeneous catalysts by applying nanofiltration techniques,^[8] as well as the use of these supramolecular scaffolds for the controlled syn-



Scheme 1. Symmetrical cationic hexa(pincer-metal) complex as template for the formation of large heterocyclic structures. FG = functional group.

thesis of macromolecular structures. These multimetallic complexes possess a high symmetry, making them promising candidates as templates in the synthesis of macromolecular heterocyclic structures. By coordinating bifunctionalized ligands to the metal centers of **A**–**C**, a pre-organization of the functional groups is attained (Scheme 1). The functional groups can now selectively react with each other, which should lead to the formation of large heterocyclic structures (as exemplified in Scheme 1 for **A** as template). The challenging step in this process is the final ring-closing reaction, since various side-reactions are anticipated, such as small intraligand ring formation, intermolecular couplings and metal-ligand dissociation. Also, the nature of the metal-to-ligand coordination bond is of crucial importance for the success of this ring-closure process. It has to be sufficiently strong under the reaction conditions in order to prevent ligand dissociation from the template. However, afterward dissociation of the macrocycle by cleavage of the metal-to-ligand interactions has to be facile as well. Regarding these aspects, olefin metathesis seems to be very promising for the crucial ring-closing step, since it tolerates many functional groups and can be performed under rather mild reaction conditions as well. However, the use of coordination complexes in RCM has hardly been the subject of investigation. Therefore, we performed a model study with monometallic systems in order to determine the ideal conditions for this approach. In this study, diolefin-substituted pyridines were selected as the ligands because of the suitable stability of the pyridine-palladium and -platinum bonds. Here, we report the synthesis of various diolefin-substituted pyridines and the corresponding coordination pincer-palladium and -platinum complexes. Furthermore, we will discuss the behavior of these monometallic diolefin-substituted pyridine-pincer complexes in RCM.

Results and Discussion

Synthesis of Diolefin-Substituted Pyridines

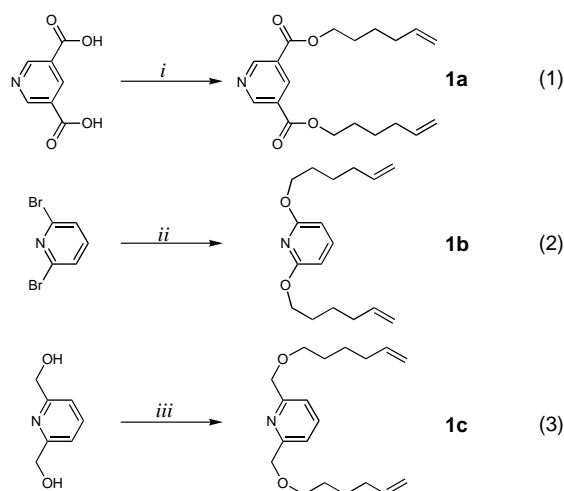
A number of diolefin-substituted pyridines were selected for this study and their syntheses are summarized in Scheme 2. We chose these symmetric pyridines because the olefinic tails are then directed in such a way that the formation of macrocycles using template-directed synthesis should be facilitated (Scheme 1). Furthermore, it enabled us to study the influence of the positioning of the olefinic tails on the pyridine rings (3,5- or 2,6-substitution) in RCM as well as the influence of a slightly longer olefinic tail (**1b** vs. **1c**). Treatment of 3,5-pyridinedicarboxylic acid with thionyl chloride and subsequent reaction of *in situ* generated diacid chloride with 5-hexenol resulted, after a basic work-up, in the

formation of **1a** (Scheme 2, equation 1). Treatment of 2,6-dibromopyridine with *in situ* prepared sodium salt of 5-hexenol in dry DMF, gave 2,6-disubstituted pyridine **1b** in 90% yield (Scheme 2, equation 2). Finally, pyridine **1c** was obtained in a two-step sequence; 2,6-pyridinedimethanol was first reacted with thionyl chloride and subsequent treatment of *in situ* formed 2,6-bis(chloromethyl)pyridine with the sodium salt of 5-hexenol yielded **1c** in 91% yield (Scheme 2, equation 3).

Preparation of Monometallic Pyridine Complexes

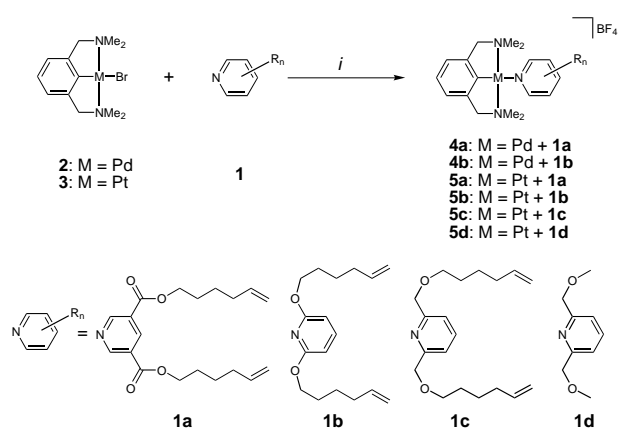
Metalated *pincer* complexes (pincer ligand: mono-anionic, terdentate coordinating ligand: $\text{YCY} = [2,6-(\text{CH}_2\text{Y})_2\text{C}_6\text{H}_3]^-$) were chosen as the organometallic moieties for coordination of the difunctionalized pyridines. Various functionalities of the pincer moiety can be altered rather easily, thus allowing fine-tuning of the material for various applications.^[9] In this investigation, we decided to use the monoanionic NCN-pincer ligand ($\text{NCN} = [2,6-(\text{CH}_2\text{NMe}_2)_2\text{C}_6\text{H}_3]^-$) in combination with palladium(II) and platinum(II) centers. In Scheme 3, the general synthetic pathway to NCN-metal-pyridine complexes is shown. Treatment of the NCN-M-Br (**2**, M = Pd; **3**, M = Pt) with AgBF_4 in CH_2Cl_2 in the presence of the appropriate diolefin-substituted pyridine, resulted in the formation of the various pincer-metal-pyridine tetrafluoroborate complexes **4a–b** and **5a–c** all in high yields.

The ^1H NMR spectra of complexes **4a–b** and **5a–b** showed the expected chemical shifts upon coordination of the pyridine moiety to the organometallic pincer complexes. For **5c**, however, ^1H NMR spectroscopy showed an unusual large downfield shift of $\Delta\delta$ 1.0 ppm



Scheme 2. *i.* SOCl_2 , reflux, 20 h followed by 5-hexenol in CH_2Cl_2 , $0^\circ\text{C} \rightarrow$ reflux, 3 h. *ii.* sodium 5-hexenolate, DMF, 95°C , 16 h. *iii.* SOCl_2 , CH_2Cl_2 , RT, 20 h, followed by sodium 5-hexenolate, THF, reflux, 16 h.

for the py-CH₂O-protons of the 2,6-disubstituted pyridine **1c** upon coordination, indicating the existence of a rather strong interaction between these protons and the platinum center. Unfortunately, crystals of **5c** suitable for an X-ray single crystal structure determination could not be obtained. In order to study the influence of the *ortho*-methylalkoxy substituents on the pyridine orientation with respect to the pincer moiety, **5d**^[10] (Scheme 3) was prepared as a model compound for **5c** and analyzed by ¹H NMR spectroscopy and X-ray single crystal structure determination (Figure 2). ¹H NMR analysis of **5d** showed the same large downfield shift of the py-CH₂O-protons of **1d** upon coordination to the platinum center. In the crystal structure of **5d**, the unit cell contains two independent cationic platinum complexes. Since the geometry of both are similar, the structural features of only one of the complexes will be discussed here. Table 1 summarizes a number of selected distances and angles for one of the independent complexes of **5d** in the solid state. As shown in Figure 2, the square-planar platinum(II) center is ligated by a terdentate η³-coordinated NCN-ligand and a η¹-N-coordinated pyridine ligand. As a result of the η³-N,C,N-coordination, C_{ipso} and N(py) are mutually *trans* orientated. The pincer aryl ring is tilted 13.21(15)° with respect to the N1-C1-N2-N3 coordination-plane, while the pyridine is fixed in a conformation that is almost



Scheme 3. *i.* AgBF₄, CH₂Cl₂, RT, 1 h.

Table 1. Interatomic bond lengths (Å) and angles (deg.) of **5d**.

Bond lengths		Bond angles	
Pt1–C1	1.935(3)	C1–Pt1–N3	179.26(13)
Pt1–N1	2.099(3)	C1–Pt1–N1	81.12(13)
Pt1–N2	2.107(3)	C1–Pt1–N2	81.31(13)
Pt1–N3	2.192(3)	N1–Pt1–N2	162.42(11)
Pt1–H18A	2.6385	N1–Pt1–N3	98.91(11)
Pt1–H20B	2.5934	N2–Pt1–N3	98.67(11)
		C18–H18A–Pt1	119.96
		C20–H20B–Pt1	124.23

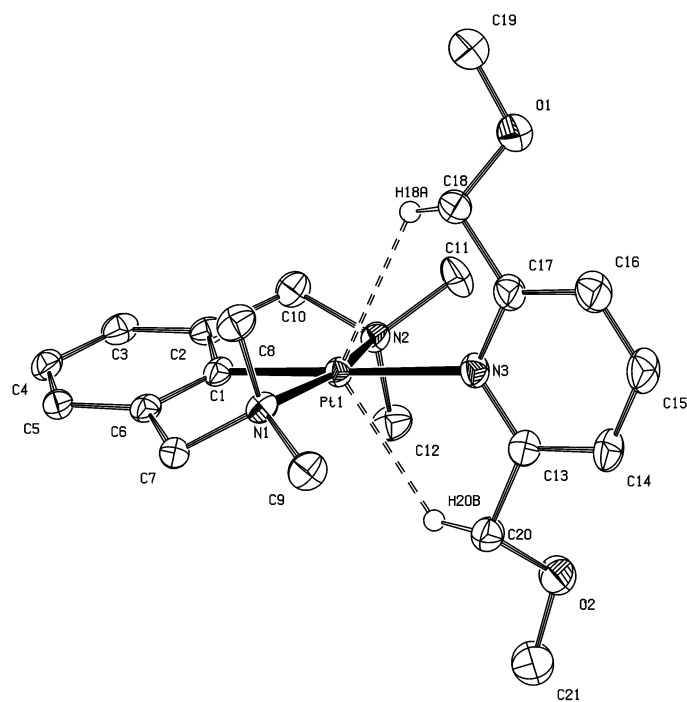
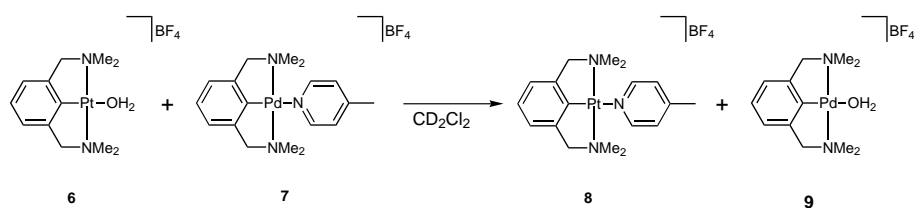


Figure 2. Crystal structure of one of the two independent **5d** cations; ORTEP 50% displacement ellipsoids; only the relevant hydrogens are shown, the tetrafluoroborate anion and co-crystallized CH₂Cl₂ are omitted for clarity.

perpendicular [87.47(16)°] to this plane. The stereochemistry, bond lengths and bond angles are normal for a square-planar platinum(II) center containing the NCN ligand.^[11] An interesting feature of the structure is the positioning of H18A and H20B near the virtual *z*-axis of the platinum center. The distances H18A–Pt1 (2.639 Å) and H20B–Pt1 (2.593 Å) are significantly shorter than the sum of the Van der Waals radii of both nuclei (3.50 Å), indicating an additional interaction with the filled *d*_{z² orbital of the platinum center, providing extra stability to this structure. The earlier mentioned large down-field shift of the py-CH₂O-protons in the ¹H NMR spectrum of **5d** in acetone-*d*₆ also suggests a similar interaction of these protons with the platinum center in solution, leading to rigid rotation of the pyridine ligand about the Pt1–N3 axis as well as to restricted rotation about the C17–C18 and C13–C20 axes. Consequently, these hydrogen nuclei undergo a down-field shift. Such behavior has been observed previously for a neutral [Pt(η³-NCN)(η¹-NCN)] complex.^[12]}

An important aspect of this research is the strength of the pyridine-metal coordination bond in the various NCN-M-py cationic complexes. First of all, for template-directed synthesis of macromolecular heterocycles using **A–C** (Figure 1) as templates, it is of crucial importance that the M-py bond is maintained during the formation of the large ring and thus has sufficient kinetic stability under the reaction conditions. Furthermore, for RCM (as the crucial ring-closing reaction) it is impor-



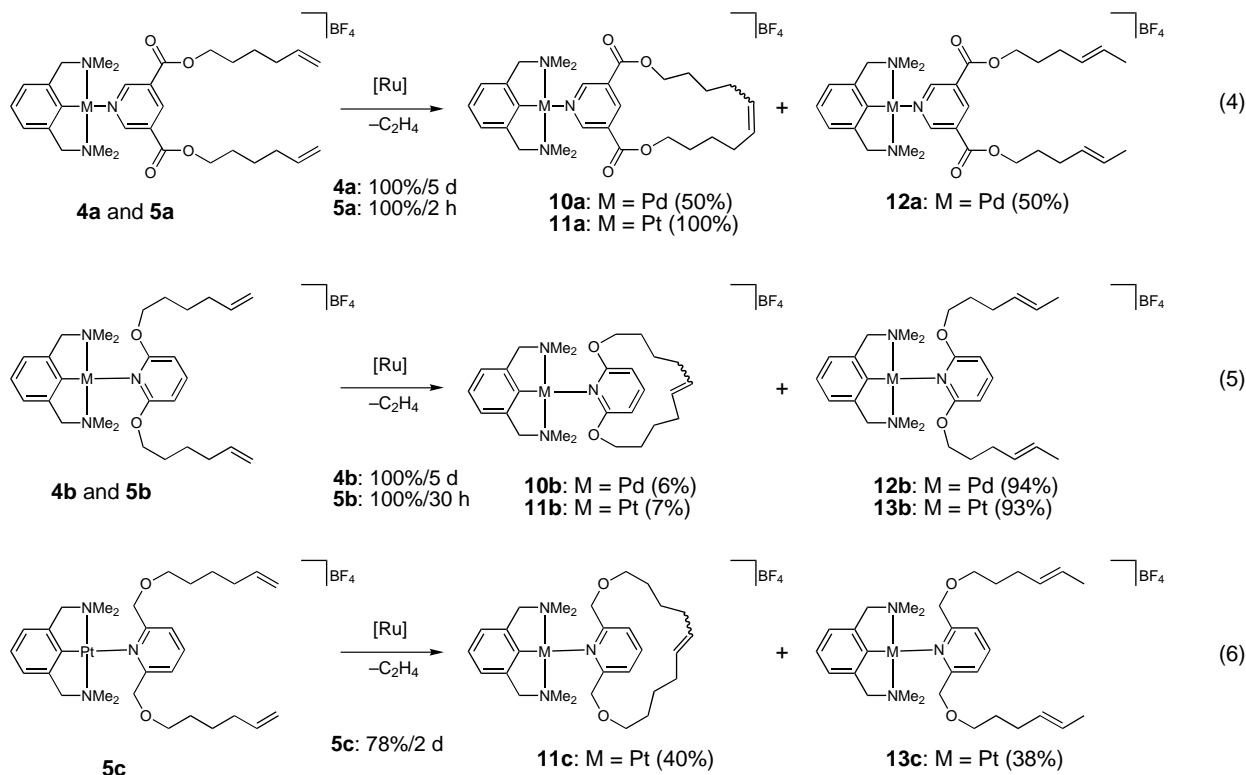
Scheme 4. 4-Picoline exchange experiment.

tant that the Lewis-basic pyridine ligands remain coordinated to the pincer-metal centers in order to prevent fast deactivation of the metathesis catalyst due to competitive coordination of free pyridine in solution to the active site of the catalyst. Therefore, we performed a number of independent ^1H NMR spectroscopy experiments with cationic NCN-M-(4-picoline) complexes (prepared similarly to the complexes shown in Scheme 3). In the first experiment, cationic NCN-Pt-aqua complex **6** was mixed in CD_2Cl_2 with the cationic NCN-Pd-(4-picoline) complex **7** at room temperature (Scheme 4). ^1H NMR spectroscopy clearly indicated the disappearance of palladium-(4-picoline) complex **7** and the quantitative formation of the platinum-(4-picoline) complex **8**, i.e., a $\Delta\delta$ of 0.15 ppm of the *ortho*-picoline protons together with the appearance of platinum-couplings on the *ortho*-protons ($^3J_{\text{Pt,H}}$ = not resolved) were observed.^[13] In a second set of experiments, both NCN-Pd-(4-picoline) complex **7** and the platinum analogue **8** were separately dissolved in CD_2Cl_2 in the

presence of a 10-fold excess of 4-picoline. In the case of platinum-complex **8**, ^1H NMR spectroscopy showed two sharp resonances for coordinated and non-coordinated picoline in a 1:10 ratio, as indicated by a characteristic downfield shift of $\Delta\delta_{\text{H}}$ 0.5 ppm for the *ortho*-aromatic protons of 4-picoline upon coordination. This observation points to a slow exchange reaction for the 4-picolyl complex in solution on the NMR time-scale. As expected the corresponding palladium complex **7** undergoes a fast 4-picolyl exchange reaction, as ^1H NMR spectra showed a single resonance pattern for coordinated and free 4-picoline.

Metathesis with Diolefin-Substituted Pyridines Bound to Mononuclear Pincer-Palladium and -Platinum Complexes

Pyridine complexes **4a,b** and **5a–c** were subjected to RCM reaction conditions using the first-generation



Scheme 5. Metathesis with diolefin-substituted pyridines coordinated to palladium and platinum centers. Percent values under the arrows refer to conversion.

Grubbs' catalyst, $[(\text{Cy}_3\text{P})_2\text{Cl}_2\text{Ru}=\text{CHPh}]$. The results are summarized in Scheme 5. All metathesis reactions were performed under the same reaction conditions: 0.016 M [olefin end groups], 5 mol % [Ru] per pyridine in CH_2Cl_2 at reflux temperatures. The reaction progress was monitored by ^1H NMR spectroscopy and GC-MS. Applying these RCM reaction conditions to pyridine complexes **4a** and **5a**, resulted in the formation of the metathesized products **10a** (50%, *cis/trans* mixture) and **11a** (100%, *cis/trans* mixture) (equation 4, Scheme 5), respectively. Remarkably, the time needed for complete conversion of **4a** was found to be considerably longer (5 d) than for **5a** (2 h). Furthermore, with **4a** the isomerized product **12a** (50%) was formed in addition to the metathesis product **10a**. The formation of **12a** is due to a prototropic isomerization of the double bond, which is known to be catalyzed by transition metal complexes.^[14] The origin of the large differences observed between palladium and platinum (**4a** and **5a**, respectively) probably lies in the much higher kinetic stability of the M-N(py) coordination bond in **5a** as compared to **4a** (*vide supra*). As a consequence, in the case of palladium complex **4a**, the pyridine ligand dissociates partially from the palladium center, leading to free pyridine in solution, which can compete for the active site of the ruthenium metathesis catalyst. This leads to a decreased catalyst activity and thus to longer metathesis reaction times. Apparently, under these conditions isomerization (usually a slow reaction), which leads to the formation of internal olefinic ligands, becomes relatively more important and competitive as the RCM becomes slower.

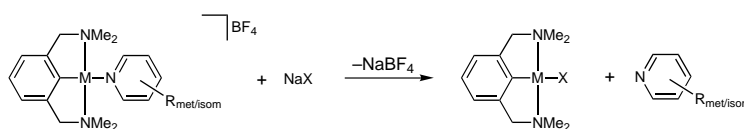
Subjecting complexes **4b** and **5b** to metathesis reaction conditions, resulted mainly in the formation of isomerized products **12b** and **13b** (> 90%; equation 5, Scheme 5), while minor amounts of metathesis products **10b** (6%) and **11b** (7%) were present. These results point to the importance of the position as well as the conformational stability of the group linking the olefinic substituents to the pyridine ring; the carbonyl linkage in **4a** and **5a**, which is coplanar with the pyridine ring and provides a 17-membered ring on ring-closing, *vs.* the ether-linkage in **4b** and **5b**, which directs the olefinic substituents less and gives a smaller ring of 15 atoms. Furthermore, **4b** and **5b** possess 2,6-diolefin-substituted pyridines, resulting in increased steric hindrance (by the pincer moiety and the pyridine ring) for the olefinic tails during RCM, forcing the ring-closing reaction to take place *via* a back-flip conformation. This will lead to a slower metathesis reaction and thus shifting the selectivity of the reaction toward the competing isomerization process. Remarkably, the reaction time needed for complete conversion of **4b** is considerably longer than for **5b** (5 days *vs.* 30 hours, respectively). Apparently, under the reaction conditions the pincer-metal moiety plays a significant role in the isomerization reaction as indicated by the large difference in isomer-

ization rates between platinum (**5b**) and palladium (**4b**). Most likely dissociation of the pyridine ligand from the pincer-metal center has to occur before the pincer moiety can take part in the isomerization process, however the exact role of the pincer moiety is not understood yet and is subject to further investigation. These results once again demonstrate that isomerization becomes a competing reaction when the reaction times for complete conversion increase.

In the final example, complex **5c** is applied in the RCM (equation 6, Scheme 5). In this case, both metathesis (**11c**) and isomerization (**13c**) take place in approximately equal ratios. The slightly longer olefin-tails (one CH_2 -group) in **5c**, as compared to **5b**, result in less ring-strain (17-membered ring), allowing metathesis to take place to a greater extent. For **5c**, both metathesis (as compared to **5a**, equation 4, Scheme 5) and isomerization (as compared to **5b**, equation 5, Scheme 5) are rather slow (78% total conversion of **5c** in 2 days). The slow metathesis reaction can be attributed to steric hindrance involved in the formation of the cyclic compound because of the positioning of the olefinic tails at the 2- and 6-positions (in **5c**) of the pyridine ligand rather than at the 3- and 5-positions (in **5a**). The slow isomerization reaction is probably caused by stronger binding of the pyridine to the NCN-Pt(II) moiety due to the additional interaction of the py- CH_2O -protons with the platinum center (also discussed for model compound **5d**, *vide supra*). This latter behavior results in a lower concentration of active Pt(II) isomerization species in solution (assuming that a pyridine-free ionic NCN-Pt(II) center takes part in the isomerization process) and thus in a slower isomerization process. In addition, a lower concentration of free pyridine in solution also results in less metathesis catalyst poisoning, which can be an additional explanation for the observed differences in metathesis between **5b** and **5c**.

Monometallic Pincer Complexes as Protecting Groups for Lewis-Basic Substituents in Olefin Metathesis

An interesting aspect of this approach is that olefins containing Lewis-basic substituents (such as nitriles, amines and pyridines) can in principle now be applied in metathesis reactions. Here, we have shown that olefin-substituted pyridines can now be applied in RCM by coordinating the Lewis-basic nitrogen-atom of the pyridine to a Lewis-acidic pincer-metal center prior to metathesis. The protecting organometallic pincer moiety has the advantage that it can be very easily cleaved off by addition of NaX ($\text{X} = \text{Cl}, \text{Br}, \text{I}$) to a solution of the pincer-metal-pyridine complex, affording the free pyridine and the neutral NCN-M-X complex (Scheme 6). The neutral pincer complex can subsequently be isolated and reused (*cf.* Scheme 3). We believe that this



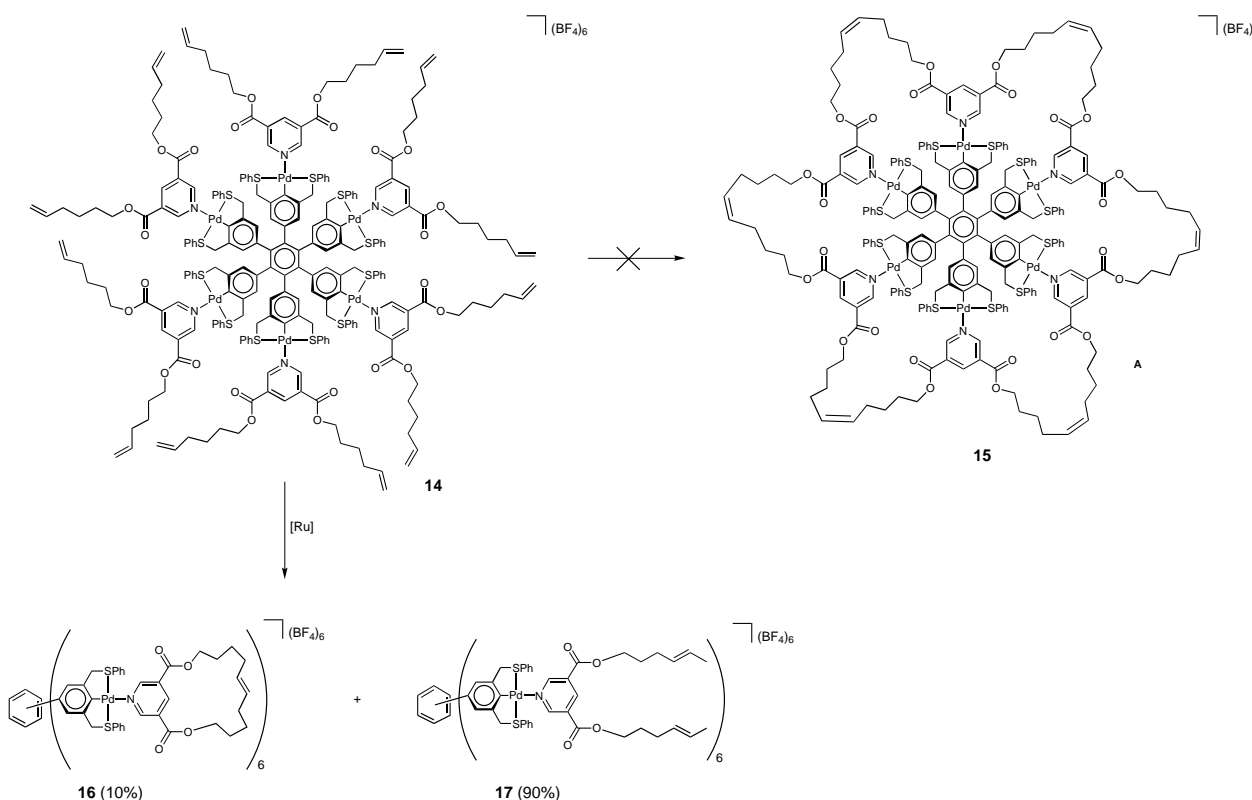
Scheme 6. Decomplexation of the pyridine-product by NaCl, NaBr or NaI.

approach can generally be applied to metathesize various olefinic compounds containing Lewis-basic substituents. In addition, since basic substituents are often not tolerated in many other catalytic reactions as well, this approach of using transition-metal complexes, e.g., the cationic NCN-Pt-center, as protecting groups during catalysis can be of general interest. Currently, we are investigating the scope of this approach.

Metathesis with a Diolefin-Substituted Pyridine Bound to a Hexakis(SCS-Pd^{II}) Template

Preliminary experiments with 3,5-diolefin-substituted pyridine **1a** connected to hexa-cationic hexakis[SCS-Pd(II)] template **14** (Scheme 7) in RCM (using 5 mol % of [Ru] per pyridine), did not result in the formation of the desired macrocycle **15**. Instead mainly isomerized product **17** was obtained, while only minor amounts of intrapyridyl metathesis product **16** were observed

(**16:17** = 1:9, complete conversion of **14** in 36 h). When these results are compared to the results obtained with NCN-Pd-pyridine complex **4a** (equation 4, Scheme 5), it is clear that the isomerization reaction is considerably faster in the case of **14** (5 d vs. 36 h for complete conversion). Metathesis, on the other hand, is almost completely suppressed with **14** under the reaction conditions. Apparently, the palladium-pyridine bond in **14**, i.e., in each of the six cationic SCS-Pd-pyridine units, is weaker than in **4a**. Consequently, it can be assumed that the high concentration of free diolefinic-pyridine ligand **1a** in solution results in more effective metathesis-catalyst poisoning and thus in almost no RCM product formation. Moreover, the free SCS-Pd cationic sites are apparently effective catalytic sites for the olefin isomerization process (*vide supra*). These assumptions were confirmed by independent experiments in which **4a** and its mononuclear SCS-Pd-pyridine analogue (SCS = [C₆H₃(CH₂SPh)₂-2,6]⁻) were dissolved in CH₂Cl₂ and stirred at room temperature for 20 hours



Scheme 7. Preliminary test toward macrocyclic structures.

(without [Ru] metathesis catalyst). The SCS-complex gave 75% isomerization of **1a** to the internal olefin in 20 hours, whereas **4a** showed no conversion at all under the same conditions. Furthermore, independent ^1H NMR spectroscopic experiments (acetone- d_6 , 200 MHz) showed a smaller downfield shift for the *ortho*-protons of the 3,5-disubstituted pyridine in **14** ($\delta_{\text{H}} = 9.08$ ppm) as compared to **4a** ($\delta_{\text{H}} = 9.67$ ppm), pointing to a stronger Pd-N(py) coordination bond in the case of **4a**. These results clearly suggest that the relatively weak SCS-Pd-pyridine bond is responsible for the almost exclusive formation of **17** in the attempted synthesis of macrocycle **15** (Scheme 7). Furthermore, the fact that in metathesis no **15** but rather **16**, albeit in small amounts, was found, reveals that with **16** intraligand RCM occurs rather than interligand RCM which would result in the formation of **15**.

Conclusion

It is obvious from the results of this study that in order to selectively form macromolecular heterocycles, such as **15**, by RCM the fast intraligand metathesis and the isomerization reaction of the olefinic substituents have to be competed for by fast interligand metathesis and slow M-N(diolefinic-pyridine) dissociation. The most promising candidate to achieve this goal using multipincer templates should comprise 2,6-diolefin-substituted pyridines bound to a multi-(NCN-Pt^{II})-template, which can subsequently undergo RCM. The latter complexes likely match low Pt-N(py) dissociation rates with low intraligand RCM reactivity of 2,6-diolefin-substituted pyridines. As an effect, interligand RCM along the periphery of the template can be successful. The preparation of the required multi-(NCN-Pt^{II})-templates and their use in the synthesis of large heterocyclic compounds is currently under investigation.

Experimental Section

All reactions were carried out using standard Schlenk techniques under an inert atmosphere of dry, oxygen-free nitrogen unless stated otherwise. All solvents were carefully dried and distilled over appropriate drying agents prior to use. All standard reagents were purchased from Acros or Aldrich. $\text{C}_6\text{H}_3\{\text{PdBr}\}\text{-1-(CH}_2\text{NMe}_2)_2\text{-3,5}$ (**2**),^[15] $\text{C}_6\text{H}_3\{\text{PtBr}\}\text{-1-(CH}_2\text{NMe}_2)_2\text{-3,5}$ (**3**),^[16] and 2,6-bis(methoxymethyl)pyridine (**1d**)^[10] were prepared according to literature procedures. ^1H (200 or 300 MHz) and ^{13}C (50 or 75 MHz) NMR spectra were recorded on a Varian AC200 or Varian 300 MHz spectrometer at 25 °C, chemical shifts are in ppm referenced to residual solvent resonances. GC-MS analysis was performed using the following conditions: column: PE-17; 30 m \times 0.32 mm² = 50 μm film thickness; gas chromatograph: Perkin-Elmer Autosystem XL; mass spectrometer: Perkin Elmer Turbomass.

Synthesis of Bis(5-hexenyl) 3,5-Pyridinedicarboxylate (**1a**)

3,5-Pyridinedicarboxylic acid (1.0 g, 6.0 mmol) was suspended in SOCl_2 (4.4 mL, 60.0 mmol) and this mixture was heated to reflux for 20 h. Subsequently, excess SOCl_2 was evaporated under vacuum and the remaining white solid was dissolved in CH_2Cl_2 (20 mL). Next, 5-hexenol (1.16 mL, 18.0 mmol) was added to this solution at 0 °C, the solution was allowed to warm to room temperature and was subsequently heated to reflux for 3 h. After removal of all volatiles under vacuum, the off-white residue was washed several times with hexanes until a white solid was obtained. This solid was dissolved in CH_2Cl_2 (20 mL) and washed with aqueous NaOH (1 M, 50 mL). The organic layer was collected and dried (MgSO_4). After filtration and evaporation of the solvent, the crude product was flame-distilled, resulting in a yellow viscous oil; yield: 1.3 g (65%); ^1H NMR (C_6D_6 , 300 MHz): $\delta = 9.43$ (d, $^4J_{\text{H,H}} = 3.3$ Hz, 2H, ArH), 8.87 (t, $^4J_{\text{H,H}} = 3.3$ Hz, 1H, ArH), 5.61 (m, 2H, $\text{CH}_2=\text{CH}$), 4.94 (m, 4H, $\text{CH}=\text{CH}_2$), 4.01 (t, $^3J_{\text{H,H}} = 9.6$ Hz, 4H, OCH_2), 1.80 (m, 4H, CH_2), 1.36 (m, 4H, CH_2), 1.15 (m, 4H, CH_2); ^{13}C NMR (acetone- d_6 , 50 MHz): $\delta = 164.80, 154.47, 139.19, 137.85, 127.09, 115.17, 66.19, 33.96, 28.75, 25.95$; anal. calcd. for $\text{C}_{16}\text{H}_{25}\text{NO}_4$: C 68.86, H 7.60, N 4.23%; found: C 68.72, H 7.68, N, 4.35%.

Synthesis of 2,6-Bis(5-hexenoxy)pyridine (**1b**)

5-Hexenol (3.7 mL, 30.0 mmol) was dissolved in THF (40 mL) and sodium (0.72 g, 30 mmol) was added in small portions. The reaction mixture was stirred until all sodium was dissolved. Subsequently all volatiles were evaporated, yielding a white solid. 2,6-Dibromopyridine (2.4 g, 8.7 mmol) dissolved in dry degassed DMF (20 mL) was added to the solid and the resulting reaction mixture was stirred overnight at 95 °C. The mixture was subsequently hydrolyzed by addition of H_2O (5 mL) and the resulting mixture was evaporated to dryness. The solid residue was dissolved in H_2O (20 mL) and the aqueous layer was extracted with Et_2O (3 \times 20 mL). The combined organic layers were dried (MgSO_4), filtered and evaporated to dryness, affording a yellow oil. This oil was flame-distilled under reduced pressure, giving a colorless oil; yield: 2.5 g (90%); ^1H NMR (acetone- d_6 , 200 MHz): $\delta = 7.54$ (t, $^3J_{\text{H,H}} = 8.0$ Hz, 1H, ArH), 6.27 (d, $^3J_{\text{H,H}} = 8.0$ Hz, 2H, ArH), 5.84 (m, 2H, $\text{CH}_2=\text{CH}$), 4.98 (m, 4H, $\text{CH}=\text{CH}_2$), 4.29 (t, $^3J_{\text{H,H}} = 6.2$ Hz, 4H, OCH_2), 2.11 (m, 4H, CH_2), 1.76 (m, 4H, CH_2), 1.55 (m, 4H, CH_2); ^{13}C NMR (acetone- d_6 , 50 MHz): $\delta = 163.65, 141.82, 139.42, 114.97, 101.91, 66.11, 34.16, 29.34, 26.17$; anal. calcd. for $\text{C}_{18}\text{H}_{26}\text{NO}_2$: C 74.14, H 9.15, N 5.09%; found: C 73.97, H 9.04, N 5.14%.

Synthesis of 2,6-Bis(5-hexenoxymethyl)pyridine (**1c**)

2,6-Pyridinedimethanol (1.2 g, 8.9 mmol) was suspended in CH_2Cl_2 (20 mL) and SOCl_2 (1.6 mL, 21.6 mmol) was added dropwise at room temperature. The reaction mixture was stirred overnight and subsequently all volatiles were evaporated under vacuum, leaving a white solid. This solid was added to a freshly prepared solution of the sodium salt of 5-hexenol [from Na (0.65 g, 28 mmol) and 5-hexenol (3.5 mL, 28 mmol) in THF, *vide supra*] in THF (50 mL) and this mixture was

heated to reflux overnight. Next, the mixture was allowed to cool to room temperature and H₂O (1.0 mL) was added. Subsequently, the reaction mixture was evaporated to dryness, the residue was dissolved in H₂O (50 mL) and the aqueous layer was extracted with Et₂O (3 × 50 mL). The combined organic layers were dried (MgSO₄) and evaporated to dryness, leaving a yellow oil. This oil was flame-distilled under reduced pressure, giving a light yellow oil; Yield: 2.46 g (91%); ¹H NMR (acetone-*d*₆, 200 MHz): δ = 7.78 (d, ³J_{H,H} = 7.8 Hz, 1H, ArH), 7.35 (d, ³J_{H,H} = 7.8 Hz, 2H, ArH), 5.85 (m, 2H, CH₂=CH), 4.98 (m, 4H, CH=CH₂), 4.54 (s, 4H, py-CH₂), 3.57 (t, ³J_{H,H} = 3.0 Hz, 4H, OCH₂), 2.07 (m, 4H, CH₂), 1.56 (m, 8H, CH₂); ¹³C NMR (acetone-*d*₆, 50 MHz): δ = 159.17, 139.52, 137.64, 120.00, 114.84, 74.26, 71.23, 34.20, 29.93, 26.25; anal. calcd. for C₂₀H₃₀NO₂: C 75.21, H 9.63, N 4.62%; found: C 75.06, H 9.55, N 4.71%.

Synthesis of 4 and 5, Typical Procedure

The appropriate combination of NCN-metal complex (0.37 mmol) and diolefin-substituted pyridine (0.75 mmol) were dissolved in CH₂Cl₂ (10 mL). A solution of AgBF₄ (72.0 mg, 0.37 mmol) in H₂O (0.2 mL) was added and the resulting suspension was stirred at room temperature for 1 h. Subsequently, the reaction mixture was filtered over Celite and the filtrate was evaporated to dryness. The obtained sticky solid was washed with hexanes to remove residual non-coordinated pyridine. After drying under vacuum, the desired products were isolated as yellowish/white solids or as a sticky residue (**5c**) and immediately used without further purification.

4a: Yield: 0.24 g (89%); ¹H NMR (acetone-*d*₆, 200 MHz): δ = 9.67 (s, 2H, ArH), 8.91 (s, 1H, ArH), 7.07 (t, ³J_{H,H} = 7.2 Hz, 1H, ArH), 6.91 (d, ³J_{H,H} = 7.2 Hz, 2H, ArH), 5.85 (m, 2H, CH₂=CH), 4.98 (m, 4H, CH=CH₂), 4.44 (t, ³J_{H,H} = 6.6 Hz, 4H, OCH₂), 4.22 (s, 4H, NCH₂), 2.83 (s, 12H, NCH₃), 2.13 (m, 4H, CH₂), 1.83 (m, 4H, CH₂), 1.60 (m, 4H, CH₂).

4b: Yield: 0.17 g (80%); ¹H NMR (acetone-*d*₆, 200 MHz): δ = 8.06 (t, ³J_{H,H} = 8.0 Hz, 1H, ArH), 7.06 (t, ³J_{H,H} = 6.6 Hz, 1H, ArH), 6.88 (m, 4H, ArH), 5.76 (m, 2H, CH₂=CH), 4.88 (m, 4H, CH=CH₂), 4.41 (t, ³J_{H,H} = 6.2 Hz, 4H, OCH₂), 4.14 (s, 4H, NCH₂), 2.85 (s, 12H, CH₃N), 2.10 (m, 8H, CH₂), 1.88 (m, 4H, CH₂), 1.51 (m, 4H, CH₂).

5a: Yield: 0.27 g (92%); ¹H NMR (acetone-*d*₆, 300 MHz): δ = 9.82 (d, ⁴J_{H,H} = 1.4 Hz, 2H, ArH), 9.00 (t, ⁴J_{H,H} = 1.4 Hz, 1H, ArH), 7.07 (t, ³J_{H,H} = 5.4 Hz, 1H, ArH), 6.96 (d, ³J_{H,H} = 5.4 Hz, 2H, ArH), 5.84 (m, 2H, CH₂=CH), 4.98 (m, 4H, CH=CH₂), 4.47 (t, ³J_{H,H} = 6.9 Hz, 4H, OCH₂), 4.33 (s, ³J_{Pt,H} = 24.9 Hz, 4H, NCH₂), 2.94 (s, ³J_{Pt,H} = 19.5 Hz, 12H, NCH₃), 2.15 (m, 4H, CH₂), 1.86 (m, 4H, CH₂), 1.58 (m, 4H, CH₂).

5b: Yield: 0.23 g (93%); ¹H NMR (acetone-*d*₆, 200 MHz): δ = 8.12 (t, ³J_{H,H} = 8.4 Hz, 1H, ArH), 6.97 (m, 5H, ArH), 5.75 (m, 2H, CH₂=CH), 4.86 (m, 4H, CH=CH₂), 4.39 (t, ³J_{H,H} = 6.2 Hz, 4H, OCH₂), 4.21 (s, ³J_{Pt,H} = 26.0 Hz, 4H, NCH₂), 2.89 (s, ³J_{Pt,H} = 19.0 Hz, 12H, NCH₃), 2.11 (m, 4H, CH₂), 2.04 (m, 4H, CH₂), 1.84 (m, 4H, CH₂).

5c: Yield: quantitative; ¹H NMR (acetone-*d*₆, 200 MHz): δ = 8.27 (t, ³J_{H,H} = 8.0 Hz, 1H, ArH), 7.91 (d, ³J_{H,H} = 8.0 Hz, 2H, ArH), 7.02 (m, 3H, ArH), 5.80 (s, 4H, py-CH₂), 5.78 (m, 2H, CH₂=CH), 4.94 (m, 4H, CH=CH₂), 4.32 (s, ³J_{Pt,H} = 26.4 Hz, 4H, NCH₂), 3.79 (t, ³J_{H,H} = 6.2 Hz, 4H, OCH₂), 2.88 (s, ³J_{Pt,H} =

20.0 Hz, 12H, NCH₃), 2.07 (m, 4H, CH₂), 1.70 (m, 4H, CH₂), 1.48 (m, 4H, CH₂).

5d: Crystals suitable for X-ray single crystal structure determination were obtained by slow diffusion of hexane into a concentrated solution of **5d** in CH₂Cl₂. Yield: 92%; ¹H NMR (acetone-*d*₆, 200 MHz): δ = 8.27 (t, ³J_{H,H} = 8.0 Hz, 1H, ArH), 7.90 (d, ³J_{H,H} = 8.0 Hz, 2H, ArH), 7.00 (m, 3H, ArH), 5.74 (s, 4H, OCH₂), 4.33 (s, ³J_{Pt,H} = 27.0 Hz, 4H, NCH₂), 3.60 (s, 6H, OCH₃), 2.87 (s, ³J_{Pt,H} = 20.3 Hz, 12H, NCH₃); anal. calcd. for C₂₁H₃₂BF₄N₃O₂Pt·(CH₂Cl₂)_{1/2}: C 37.82, H 4.87, N 6.15%; found: C 37.95, H 4.80; N 6.14%.

Synthesis of 14

Hexakis(SCS-Pd-Cl)^[8b] (0.10 g, 35 μmol) and **1a** (139 mg, 0.42 mmol) were dissolved in CH₂Cl₂ (5 mL). A solution of AgBF₄ (41 mg, 0.21 mmol) in H₂O (0.1 mL) was added and the resulting suspension was stirred at room temperature for 1 h. Subsequently, the reaction mixture was filtered over Celite and the filtrate was evaporated to dryness. The obtained sticky solid was washed with hexanes to remove residual non-coordinated pyridine. After drying under vacuum, **14** was obtained as yellowish solid and immediately used without further purification.

14: Yield: 87%; ¹H NMR (acetone-*d*₆, 200 MHz): δ = 9.22 (br s, 12H, ArH), 8.91 (m, 6H, ArH), 7.76 (m, 24H, ArH), 7.47 (m, 36H, ArH), 6.78 (br s, 12H, ArH), 5.85 (m, 12H, CH₂=CH), 5.0 (m, 24H, CH=CH₂), 4.69 (br s, 24H, SCH₂), 4.40 (t, ³J_{H,H} = 6.7 Hz, 24H, OCH₂), 2.19 (m, 24H, CH₂), 1.83 (m, 24H, CH₂), 1.58 (m, 24H, CH₂).

Typical Procedure for the Metathesis Reactions

A solution of [(Cy₃P)₂Cl₂Ru=CHPh] (3.2 mg, 3.9 μmol) and the appropriate olefin precursor (80 μmol of olefin end groups) were dissolved in dry, degassed CH₂Cl₂ (5.0 mL). This mixture was heated to reflux for 12 h. The reaction was followed by ¹H NMR spectroscopy in order to determine the full conversion times. After complete conversion, excess NaBr in H₂O (1 mL) was added and all volatiles were evaporated. The liberated pyridine products were extracted with hexanes (2 × 5 mL) and the combined organic layers were filtered and concentrated to dryness. The product mixture was analyzed by ¹H NMR spectroscopy [by monitoring the disappearance of the characteristic CH₂=CH resonance (at 5.70–5.85 ppm) and appearance of internal double bonds (at 5.40–5.70 ppm)] and by GC-MS (for determination of the ratio between isomerized and metathesis products).

Crystal Structure Determination of 5d

Colorless plates of **5d** were obtained after recrystallization in hexane/dichloromethane. Intensity data were collected for a single crystal (0.24 × 0.18 × 0.06 mm) on a Nonius KappaCCD diffractometer with rotating anode at 150 K in the range 3° ≤ 2θ (Mo Kα) ≤ 55°. Of the 37,923 reflections measured, 11,509 were unique (*R*_{int} = 0.044). An empirical absorption correction was applied using DELABS in PLATON (μ = 5.683 mm⁻¹, 0.275–0.725 transmission).^[17] The structure was solved by automated Patterson methods using DIRDIF99,^[18] and refined

on F^2 by least-squares procedures using SHELXL97.^[19] Structure validation and molecular graphics preparation were performed with the PLATON package.^[17] $2(\text{C}_{21}\text{H}_{32}\text{N}_3\text{O}_2\text{Pt}) \cdot 2(\text{BF}_4) \cdot \text{CH}_2\text{Cl}_2$, FW = 1365.70 amu, triclinic, $P\bar{1}$ (No. 2), $a = 9.1923(1)$ Å, $b = 13.8349(2)$ Å, $c = 21.0198(3)$ Å, $\alpha = 77.1163(5)^\circ$, $\beta = 79.2591(5)^\circ$, $\gamma = 80.6366(7)^\circ$, $V = 2539.67(6)$ Å³, $Z = 2$, $\rho_{\text{calc}} = 1.786$ g cm⁻³; 676 refined parameters, 389 restraints, $R(F)$ [$I > 2\sigma(I)$] = 0.0268, $wR(F^2)$ = 0.0557, GooF = 1.036, $\Delta\rho_{\text{max}} = 1.06$ e Å⁻³, $\Delta\rho_{\text{min}} = -0.74$ e Å⁻³. Crystallographic data (excluding structure factors) have been deposited with the Cambridge Crystallographic Data Centre as supplementary publication no. CCDC-179385. Copies of the data can be obtained free of charge on application to CCDC, 12 Union Road, Cambridge CB2 1EZ, UK [fax: (+44) 1223-336-033; e-mail: deposit@ccdc.cam.ac.uk].

The unit cell of **5d** contains two independent cationic platinum complexes, their respective tetrafluoroborate anions and one molecule of dichloromethane. In one of the independent cations, one ether side chain is disordered over two sets of atomic positions. One of the two independent anions is also disordered. All non-hydrogen atoms were refined with anisotropic displacement parameters, but the displacement parameters of the disordered atoms were restrained to be approximately isotropic. Hydrogen atoms were constrained to idealized geometries and allowed to ride on their carrier atoms with an isotropic displacement parameter related to the equivalent displacement parameter of their carrier atoms. The tetrafluoroborate anions were restrained to approximately tetrahedral geometries.

Acknowledgements

This work was supported by the Council for Chemical Sciences of The Netherlands Organisation for Scientific Research (CW/NWO) and the Netherlands Research School Combination Catalysis (NRSC-C).

References and Notes

- [1] a) K. J. Ivin, J. C. Mol, *Olefin Metathesis and Metathesis Polymerisation*, Academic Press, New York, **1997**; b) *Topics in Organomet. Chem.*, (Ed.: A. Fürstner), Springer, Berlin, **1998**, vol. I.
- [2] a) R. R. Schrock, J. S. Murdzek, G. C. Bazan, J. Robbins, M. DiMare, M. O'Regan, *J. Am. Chem. Soc.* **1990**, *112*, 3875; b) P. Schwab, M. B. France, J. W. Ziller, R. H. Grubbs, *Angew. Chem. Int. Ed.* **1995**, *34*, 2039.
- [3] H. E. Blackwell, D. J. O'Leary, A. K. Chatterjee, R. A. Washenfelder, D. A. Bussmann, R. H. Grubbs, *J. Am. Chem. Soc.* **2000**, *122*, 58.
- [4] T. M. Trnka, R. H. Grubbs, *Acc. Chem. Res.* **2001**, *34*, 18.
- [5] B. Mohr, M. Weck, J. -P. Sauvage, R. H. Grubbs, *Angew. Chem. Int. Ed. Engl.* **1997**, *36*, 1308.
- [6] a) J. M. Martín-Alvarez, F. Hampel, A. M. Arif, J. A. Gladysz, *Organometallics* **1999**, *18*, 955; b) E. B. Bauer, J. Ruwwe, J. M. Martín-Alvarez, T. B. Peters, J. C. Bohling, F. A. Hampel, S. Szafert, T. Lis, J. A. Gladysz, *Chem. Commun.* **2000**, 2261; c) J. Ruwwe, J. M. Martín-Alvarez, C. R. Horn, E. B. Bauer, S. Szafert, T. Lis, F. Hampel, P. C. Cagle, J. A. Gladysz, *Chem. Eur. J.* **2001**, *7*, 3931.
- [7] P. L. Ng, J. Lambert, *Synlett* **1999**, 1749.
- [8] a) H. P. Dijkstra, P. Steenwinkel, D. M. Grove, M. Lutz, A. L. Spek, G. van Koten, *Angew. Chem. Int. Ed.* **1999**, *38*, 2185; b) H. P. Dijkstra, M. D. Meijer, J. Patel, R. Kreiter, G. P. M. van Klink, M. Lutz, A. L. Spek, A. J. Canty, G. van Koten, *Organometallics* **2001**, *20*, 3159; c) H. P. Dijkstra, M. Albrecht, G. van Koten, *Chem. Commun.* **2002**, 126.
- [9] M. Albrecht, G. van Koten, *Angew. Chem. Int. Ed.* **2001**, *40*, 3750.
- [10] For the synthesis of **1d** see: J. S. Bradshaw, B. A. Jones, J. S. Gebhard, *J. Org. Chem.* **1983**, *48*, 1127.
- [11] a) E. Wehman, J. T. B. H. Jastrzebski, J. -M. Ernsting, D. M. Grove, G. van Koten, *J. Organomet. Chem.* **1988**, *353*, 145; b) J. T. B. H. Jastrzebski, G. van Koten, M. Konijn, C. H. Stam, *J. Am. Chem. Soc.* **1982**, *104*, 5490.
- [12] M. Albrecht, S. L. James, N. Veldman, A. L. Spek, G. van Koten, *Can. J. Chem.* **2001**, *79*, 709.
- [13] For this particular reaction, no changes in the chemical shifts of the protons of the pincer moieties in the ¹H NMR spectrum are observed.
- [14] Bird, *Transition Metal Intermediates in Organic Synthesis*, Academic Press, New York, **1967**, p. 69.
- [15] For **2** see: P. L. Alsters, P. J. Baesjou, M. D. Janssen, H. Kooijman, A. Sicherer-Roetman, A. L. Spek, G. van Koten, *Organometallics* **1992**, *11*, 4124.
- [16] For **3** see: D. M. Grove, G. van Koten, J. N. Louwen, J. G. Noltes, A. L. Spek, H. J. C. J. Ubbels, *J. Am. Chem. Soc.* **1984**, *106*, 6609.
- [17] A. L. Spek, *PLATON, A multipurpose crystallographic tool*, Utrecht University, The Netherlands, **2002**.
- [18] P. T. Beurskens, G. Admiraal, G. Beurskens, W. P. Bosman, S. García-Granda, R. O. Gould, J. M. M. Smits, C. Smykalla, *The DIRDIF99 Program System*, Technical Report of the Crystallography Laboratory, University of Nijmegen, The Netherlands, **1999**.
- [19] G. M. Sheldrick, *SHELXL97*, University of Göttingen, Germany, **1997**.